PROCEEDINGS OF SCIENCE

The shape of the static potential with dynamical fermions

BUW-SC 2011/08
WUB/11-21

ALPHA Collaboration

Björn Leder[*a,b] **and Francesco Knechtli**[a]
[a] *Department of Physics, Bergische Universität Wuppertal*
Gaussstr. 20, D-42119 Wuppertal, Germany
[b] *Department of Mathematics, Bergische Universität Wuppertal*
Gaussstr. 20, D-42119 Wuppertal, Germany
E-mail: leder@physik.uni-wuppertal.de

We present the analysis of the static potential extracted from Wilson loops measured on CLS ensembles generated with Wilson gauge action and $N_f = 2$ flavors of O(a) improved Wilson quarks at three different lattice spacings and a range of quark masses. The shape of the static potential at distances well below the string breaking region is studied in terms of renormalized couplings derived from the static force and its derivative. We comment on the (im)possibility of extracting the Lambda parameter at our smallest lattice spacing $a = 0.05$ fm. Finally we give an update on the scale determination through r_0.

XXIX International Symposium on Lattice Field Theory
July 10-16 2011
Squaw Valley, Lake Tahoe, California

*Speaker.

1. Introduction

In this contribution we present an analysis of the static potential on lattices generated with Wilson plaquette gauge action and $N_f = 2$ flavors of non-perturbatively $\mathcal{O}(a)$ improved Wilson quarks. Periodic boundary conditions are used for all fields apart from anti-periodic boundary conditions for the fermions in time. The static potential is extracted from measurements of the on-axis Wilson loops and can therefore only be determined for distances smaller than the string breaking distance.

2. Method

Our method to extract the static potential from HYP smeared Wilson loops has been presented in [1] and is based on two steps. In the first step all the gauge links are HYP smeared [2] using the HYP2 parameters

$$\alpha_1 = 1.0\,, \quad \alpha_2 = 1.0\,, \quad \alpha_3 = 0.5\,. \tag{2.1}$$

As the time-like links are concerned, this is equivalent to the choice of a static quark action. The binding energy of a static-light meson is $E_{\rm stat} \sim \frac{1}{a} e^{(1)} g_0^2 + \ldots$ and the HYP2 choice of smearing parameters minimizes $e^{(1)}$ [3]. The static energies $V_n(r)$ ($V_0 \equiv V$ is the static potential) depends on the static quark action. Their contribution to the expectation values of Wilson loops $W(r,T)$ of size r in one of the spatial direction and size T in the time-direction is given by

$$\langle W(r,T)\rangle \sim \sum_n c_n c_n^* \mathrm{e}^{-V_n(r)(T-2a)} \quad (\text{with } N_t \to \infty \text{ time-slices})\,. \tag{2.2}$$

The coefficients c_n depend on the choice of the space-like links. In the second step of our procedure we construct a variational basis for them. The space-like links are smeared using n_l iterations of *spatial* HYP smearing

$$\langle W(r,t)\rangle \longrightarrow C_{lm}(r,T) \tag{2.3}$$

We use a basis of $l = 1,2,3$ operators and the generalized eigenvalue method to extract V_n [4, 5]. The error analysis is based on the method of [6] and we add a tail to the autocorrelation function to account for the slow modes [7].

In this contribution we mainly present results for two lattice sets at approximately constant pseudo-scalar mass $r_0 M_{\rm PS} \approx 0.62 \ldots 0.64$:

$$\text{F7a: 701 configurations}\,, \quad 96 \times 48^3\,, \quad r_0/a(\text{F7a}) = 7.079(63)\,, \tag{2.4}$$

$$\text{O7: 740 configurations}\,, \quad 128 \times 64^3\,, \quad r_0/a(\text{O7}) = 9.63(12)\,. \tag{2.5}$$

In the left plot of Fig. 1 we show the two potentials renormalized by subtracting twice the energy of a static-light meson. The right plot of Fig. 1 compares the potentials on the A5a, E5g and N5 lattices [8] computed with two different sets of HYP parameters for the static action: the HYP2 set in Eq. (2.1) and the set called HYP [2]. The difference of the potentials is

$$r_0\,[V^{\rm HYP2}(r) - V^{\rm HYP}(r)] \;=\; 2\,r_0\,(E_{\rm stat}^{\rm HYP2} - E_{\rm stat}^{\rm HYP}) + \frac{a^2\,r_0}{r^3}\,G(\Lambda r, m_q r)\,. \tag{2.6}$$

The dotted lines and gray bands represent the values with errors of $2\,r_0\,(E_{\rm stat}^{\rm HYP2} - E_{\rm stat}^{\rm HYP})$. We observe small cut-off effects encoded in the function G in Eq. (2.6).

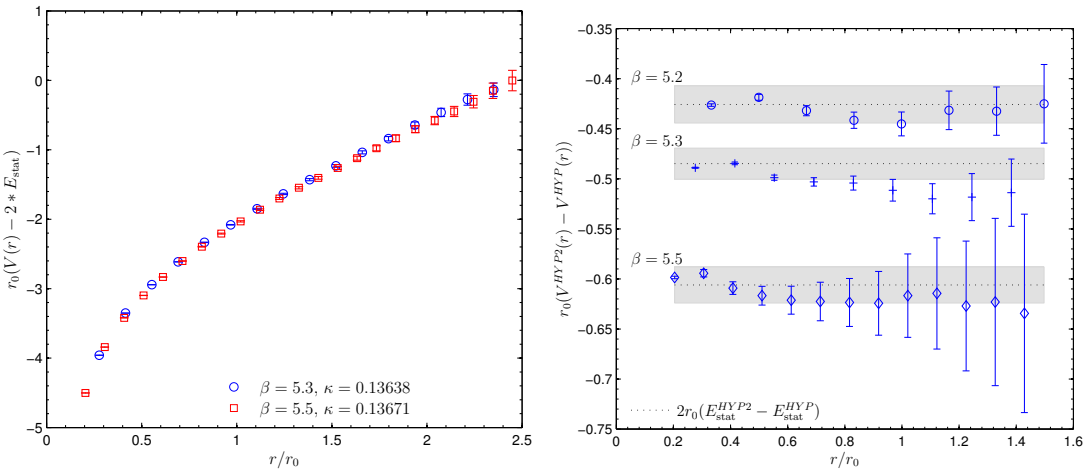

Figure 1: Left plot: the static potentials on the F7a and O7 lattices. Right plot: a comparison of the potentials using two static actions on the A5a, E5g and N5 lattices.

3. Scale r_0/a

Here we present a preliminary update on the determination of the scale r_0 [9] at the three available β values and based on the currently available statistics. Motivated by the right plot of fig. 2 we perform a combined linear extrapolation in the square of the pseudo-scalar mass to the chiral limit and obtain the following results for $r_0/a(\beta)$:

$$r_0/a(5.2) = 6.159(78)\,, \qquad r_0/a(5.3) = 7.242(70)\,, \qquad r_0/a(5.5) = 9.84(13)\,. \tag{3.1}$$

With these values of r_0/a the preliminary update of the ALPHA result for the Λ parameter extracted from the running of the Schrödinger Functional coupling [10] is

$$r_0\,\Lambda^{N_{\rm f}=2}_{\overline{\rm MS}} \;=\; 0.78(3)(5)\,. \tag{3.2}$$

The final numbers will be given in [8]. Alternative methods for determining the lattice spacing in the CLS consortium are presented at this conference, through the kaon decay constant $F_{\rm K}$ [11] or the Ω mass [12].

4. Mass dependence and cutoff effects in r_0

In order to discuss the mass dependence and cut-off effects in r_0, we introduce the variable $x = (r_0 M_{\rm PS})^2$, where $M_{\rm PS}$ is the pseudo-scalar mass, and define a reference value $r_0|_{\rm ref}$, which corresponds to the value of r_0 at the pseudo-scalar mass

$$x_{\rm ref} \equiv (r_0 M_{\rm PS})^2|_{\rm ref} \;=\; 0.75\,. \tag{4.1}$$

In the left plot of Fig. 2 we plot $r_0/r_0|_{\rm ref}$ versus x and compare our data with the twisted mass data of [13]. The value of $r_0|_{\rm ref}$ is obtained by linear interpolation and the error analysis of $r_0/r_0|_{\rm ref}$ takes into account the correlations between the data. We only consider data with $x \leq 1.2$.

Using the data plotted in the left plot of Fig. 2, we determine for each β value the slope $s(a/r_0|_{\rm ref})$ in the Taylor expansion

$$\frac{r_0}{r_0|_{\rm ref}}(x) \;=\; 1 + s(a/r_0|_{\rm ref}) \cdot (x - x_{\rm ref})\,. \tag{4.2}$$

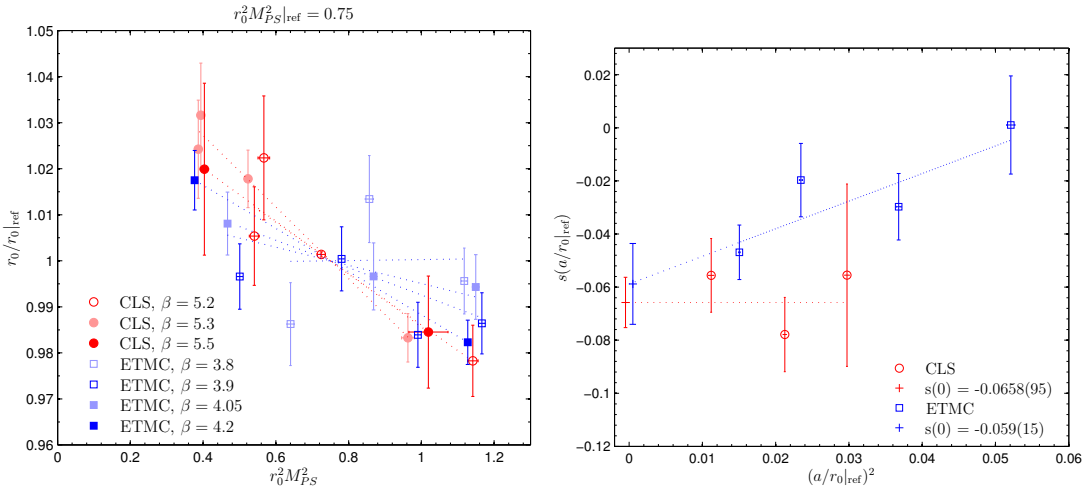

Figure 2: Left plot: mass and cut-off dependence of r_0. Right plot: continuum extrapolation of the slope $s(a/r_0|_{\rm ref})$. Comparison with twisted mass data from [13].

The results are shown in the right plot of Fig. 2. In principle they depend on the chosen value of $x_{\rm ref} = 0.75$. We repeated the analysis using $x_{\rm ref} = 0.6$ but the slopes do not change significantly. The twisted mass results for $s(a/r_0|_{\rm ref})$ increase in magnitude as $a \to 0$ and they line up with our results at the smallest a. Our data do not show significant cut-off effects and we emphasize that the errors are larger due to accounting for the slow modes in the autocorrelation function. In the continuum limit we obtain the value $s(0) = -0.0658(95)$ by fitting to a constant.

5. Running couplings

The static force $F(r) = V'(r)$ defines the running coupling in the qq-scheme $\bar{g}_{\rm qq}$ through

$$\bar{g}^2_{\rm qq}(\mu) \;=\; \frac{4\pi}{C_{\rm F}} r^2 F(r)\,,\; \mu = 1/r\,. \tag{5.1}$$

We use an improved lattice definition of F which removes the cut-off effect effects at tree level [1]. The results for $\alpha_{\rm qq}(1/r) = \bar{g}^2_{\rm qq}/(4\pi)$ on the F7a and O7 lattices are plotted in the left plot of Fig. 3. The magenta dashed and continued lines are the 3- and 4-loop running respectively. They are obtained by solving the renormalization group (RG) equation, which for a given scheme S reads (here S=qq)

$$\frac{\Lambda_{\rm S}}{\mu} \;=\; \left(b_0 \bar{g}^2_{\rm S}\right)^{-b_1/(2b_0^2)} {\rm e}^{-1/(2b_0\bar{g}^2_{\rm S})} \exp\left\{ -\int_0^{\bar{g}_{\rm S}} {\rm d}x \left[\frac{1}{\beta_{\rm S}(x)} + \frac{1}{b_0 x^3} - \frac{b_1}{b_0^2 x} \right] \right\}. \tag{5.2}$$

For the beta function $\beta_{\rm S}$ we use the 3- and 4-loop approximations [18, 19, 20, 21] and $r_0\Lambda_{\rm S}$ is calculated from the value in Eq. (3.2) [1]. One sees that our smallest lattice spacing is not small enough to make contact with perturbation theory. This becomes more evident by the attempt to determine the Λ parameter through Eq. (5.2) shown in Fig. 4. We use the $\alpha_{\rm qq}(1/r)$ values measured on the O7 lattices as input for the right hand side of Eq. (5.2) together with the perturbative beta function (2-loop, filled circles; 3-loop filled squares; 4-loop filled diamonds) and calculate $r_0\Lambda_{\overline{\rm MS}}$. For $\alpha_{\rm qq}(1/r) \to 0$ the values for the different loop approximations should converge to one value, but

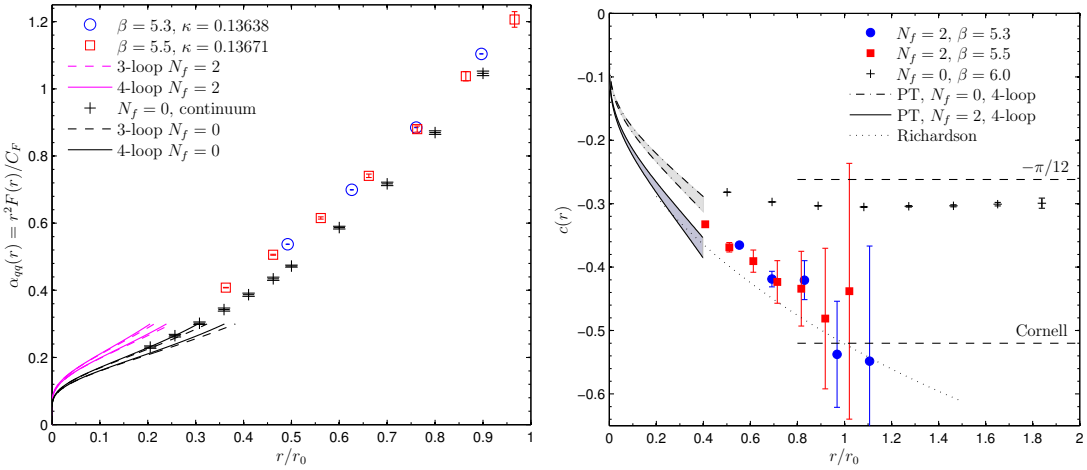

Figure 3: Left plot: the coupling $\alpha_{\rm qq}(1/r)$ compared to perturbation theory and $N_{\rm f} = 0$ results from [14]. Right plot: the slope $c(r)$ compared to perturbation theory, potential models and $N_{\rm f} = 0$ results from [15].

this is not the case for our data in Fig. 4 (note that there is no sign of the 2-loop data bending toward the 3- and 4-loop ones). For comparison we plot the $N_{\rm f} = 0$ data from [14] which demonstrate that couplings down to at least $\alpha_{\rm qq}(1/r) \approx 0.2$ (half the value of our smallest coupling on the O7 lattice) would be needed.

From the slope

$$c(r) = \frac{1}{2} r^3 F'(r) \tag{5.3}$$

the running coupling $\bar{g}_{\rm c}$ is obtained

$$\bar{g}_{\rm c}^2(\mu) = -\frac{4\pi}{C_{\rm F}} c(r), \; \mu = 1/r, \tag{5.4}$$

which defines the c-scheme. The results on the F7a and O7 lattices are plotted in the right plot of Fig. 3. We also plot the $N_{\rm f} = 0$ data from [15] showing that there is a large effect originating from dynamical fermions (at distances much below the string breaking distance), as already indicated by the perturbative curves. For comparison we plot the values of $c(r)$ calculated using two phenomenological potential models: the Cornell potential [16]

$$V_{\rm Cl} = -\frac{\kappa}{r} + \sigma r, \quad \kappa = 0.52 \tag{5.5}$$

and the Richardson potential [17]

$$V_{\rm R}(r) = \frac{1}{6\pi b_0} \Lambda \left(\Lambda r - \frac{f(\Lambda r)}{\Lambda r} \right). \tag{5.6}$$

If $r\Lambda \ll 1$, $V_{\rm R}(r) \sim -1/[6\pi b_0 r \ln(1/\Lambda r)]$, where b_0 is the 1-loop coefficient of the beta function. If $r\Lambda \gg 1$, $V_{\rm R}(r) \sim \text{const} \times r$. Our data seem to follow the Richardson curve (dotted line, $N_{\rm f} = 2$, $r_0\Lambda = 0.73$) and approach the Cornell value at distances around r_0, where unfortunately the statistical errors (enhanced by the factor r^3) become too large.

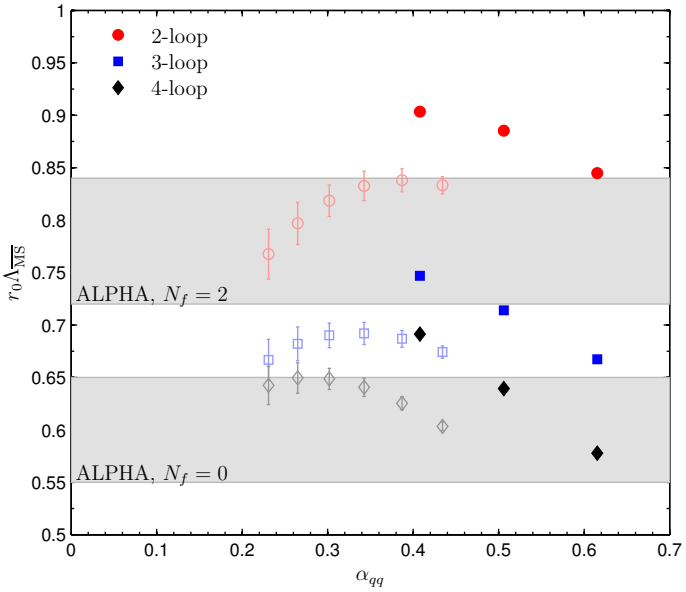

Figure 4: Attempt to extract the Λ parameter solving the RG equation for $\alpha_{\rm qq}(1/r)$ with the 2-, 3- and 4-loop β function. $N_{\rm f} = 0$ data are from [14].

6. Conclusions

We determine the static potential from Wilson loops using the HYP2 static action. Cut-off effects in the potential appear to be small and r_0/a can be accurately determined. There could be non-negligible cut-off effects in the mass dependence of r_0 [22], however they seem to be small with improved Wilson fermions.

The running coupling from the static force is compared to perturbation theory: at our lattice spacing we cannot reach small enough distances in order to extract the Λ parameter. This is in contrast to what is concluded by a recent work with the same lattice spacing [23]. We observe large effects from dynamical fermions in the slope $c(r)$. The shape of the static potential is relevant for holographic QCD models [24, 25].

Acknowledgements

We thank Rainer Sommer for helpful discussions on various aspects of this work. We further thank the Forschungszentrum Jülich and the Zuse Institute Berlin for allocating computing resources to this project. Part of the Wilson loop measurements were performed on the PC-cluster of DESY, Zeuthen.

References

[1] M. Donnellan, F. Knechtli, B. Leder, R. Sommer, *Determination of the Static Potential with Dynamical Fermions*, *Nucl. Phys. B* **849** (2011) 45.

[2] A. Hasenfratz, F. Knechtli, *Flavor symmetry and the static potential with hypercubic blocking*, *Phys. Rev. D* **64** (2001) 034504.

[3] M. Della Morte, A. Shindler, R. Sommer, *On lattice actions for static quarks*, *JHEP* **0508** (2005) 051.

[4] M. Lüscher, U. Wolff, *How To Calculate The Elastic Scattering Matrix In Two-dimensional Quantum Field Theories By Numerical Simulation*, *Nucl. Phys. B* **339** (1990) 222.

[5] B. Blossier, M. Della Morte, G. von Hippel, T. Mendes, R. Sommer, *On the generalized eigenvalue method for energies and matrix elements in lattice field theory*, *JHEP* **0904** (2009) 094.

[6] U. Wolff, *Monte Carlo errors with less errors*, *Comput. Phys. Commun.* **156** (2004) 143, Erratum-ibid.176:383,2007.

[7] S. Schaefer, R. Sommer, F. Virotta, *Critical slowing down and error analysis in lattice QCD simulations*, *Nucl. Phys. B* **845** (2011) 93.

[8] P. Fritzsch, F. Knechtli, B. Leder, M. Marinkovic, S. Schaefer, R. Sommer, F. Virotta, in preparation.

[9] R. Sommer, *A New way to set the energy scale in lattice gauge theories and its applications to the static force and α_s in SU(2) Yang-Mills theory*, *Nucl. Phys. B* **411** (1994) 839-854.

[10] M. Della Morte, R. Frezzotti, J. Heitger, J. Rolf, R. Sommer, U. Wolff, *Computation of the strong coupling in QCD with two dynamical flavors*, *Nucl. Phys. B* **713** (2005) 406.

[11] M. Marinkovic, S. Schaefer, R. Sommer, F. Virotta, *Strange quark mass and Lambda parameter by the ALPHA collaboration*, PoS(Lattice 2011)232.

[12] S. Capitani, M. Della Morte, G. von Hippel, B. Knippschild, H. Wittig, *Scale setting via the Ω baryon mass*, [arXiv:1110.6365], these proceedings.

[13] R. Baron *et al.* [ETM Collaboration], *Light Meson Physics from Maximally Twisted Mass Lattice QCD*, *JHEP* **1008** (2010) 097.

[14] S. Necco, R. Sommer, *The $N_f = 0$ heavy quark potential from short to intermediate distances*, *Nucl. Phys. B* **622** (2002) 328.

[15] M. Lüscher, P. Weisz, *Quark confinement and the bosonic string*, *JHEP* **0207** (2002) 049.

[16] E. Eichten, K. Gottfried, T. Kinoshita, K. D. Lane, T. -M. Yan, *Charmonium: Comparison with Experiment*, *Phys. Rev. D* **21** (1980) 203.

[17] J. L. Richardson, *The Heavy Quark Potential and the Upsilon, J/psi Systems*, *Phys. Lett. B* **82** (1979) 272.

[18] N. Brambilla, A. Pineda, J. Soto, A. Vairo, *The Infrared behavior of the static potential in perturbative QCD*, *Phys. Rev. D* **60** (1999) 091502.

[19] N. Brambilla, A. Pineda, J. Soto, A. Vairo, *Potential NRQCD: An Effective theory for heavy quarkonium*, *Nucl. Phys. B* **566** (2000) 275.

[20] A. V. Smirnov, V. A. Smirnov, M. Steinhauser, *Three-loop static potential*, *Phys. Rev. Lett.* **104** (2010) 112002.

[21] C. Anzai, Y. Kiyo, Y. Sumino, *Static QCD potential at three-loop order*, *Phys. Rev. Lett.* **104** (2010) 112003.

[22] R. Sommer *et al.* [ALPHA and CP-PACS and JLQCD Collaborations], *Large cutoff effects of dynamical Wilson fermions*, *Nucl. Phys. Proc. Suppl.* **129** (2004) 405.

[23] K. Jansen, F. Karbstein, A. Nagy, M. Wagner, *Lambda_msbar from the static potential for QCD with n_f=2 dynamical quark flavors*, [arXiv:1110.6859].

[24] U. Kol, J. Sonnenschein, *Can holography reproduce the QCD Wilson line?*, *JHEP* **1105** (2011) 111.

[25] D. Giataganas, N. Irges, *Flavor Corrections in the Static Potential in Holographic QCD*, [arXiv:1104.1623].